Experimental observation of strong edge-effects on the pseudo-diffusive transport of light in photonic graphene

Zandbergen, S.R.; Dood, M.J.A. de

Experimental Observation of Strong Edge Effects on the Pseudodiffusive Transport of Light in Photonic Graphene

Sander R. Zandbergen and Michiel J. A. de Dood*

Huygens Laboratory, Leiden University, Niels Bohrweg 2, 2333 CA Leiden, The Netherlands

(Received 15 September 2009; revised manuscript received 13 November 2009; published 29 January 2010)

Photonic graphene is a two-dimensional photonic crystal structure that is analogous to graphene. We use 5 mm diameter Al_2O_3 rods placed on a triangular lattice with a lattice constant $a = 8$ mm to create an isolated conical singularity in the photonic band structure at a microwave frequency of 17.6 GHz. At this frequency, the measured transmission of microwaves through a perfectly ordered structure enters a pseudodiffusive regime where the transmission scales inversely with the thickness L of the crystal ($L/a \gtrsim 5$). The transmission depends critically on the configuration of the edges: distinct oscillations with an amplitude comparable to the transmission are observed for structures terminated with zigzag edges, while these oscillations are absent for samples with a straight edge configuration.

DOI: 10.1103/PhysRevLett.104.043903 PACS numbers: 42.25.Gy, 42.25.Bs, 42.70.Qs

The experimental realization of graphene [1], a single layer of carbon atoms arranged in a two-dimensional hexagonal structure, has attracted a lot of attention. The interest in this gapless semiconductor is due to the conical singularities in the electronic band structure [2] that create a linear dispersion for electrons, leading to interesting physical phenomena such as an anomalous quantum Hall effect and the absence of Anderson localization [3,4]. Since the dispersion around these points is linear, the motion of electrons resembles that of massless particles and can be described by the relativistic Dirac equation. These singularities have been aptly named ''Dirac points'' and are entirely due to the geometry of the underlying triangular lattice.

As a consequence, similar conical singularities can be identified in the band structure of electromagnetic waves in two-dimensional photonic crystals with a triangular lattice [5–7], acoustic waves in a sonic crystal [8], and electrons in a two-dimensional electron gas [9]. Of these analogous systems, only the propagation of acoustic waves was studied experimentally, and an acoustic analogue to the Zitterbewegung of relativistic electrons was identified [8]. The analogy between graphene and these structures strengthens our understanding of the physics common to these two-dimensional structures. In particular, the analogy with optics has already inspired researchers to predict known optical effects, such as negative refraction [10] and a Goos-Hänchen shift for electrons in graphene [11].

Despite the success of graphene, the observation of effects predicted by theory often require samples with perfect edges of a well-defined configuration that can only be obtained by atomic scale engineering. In this Letter, we experimentally investigate a photonic crystal structure for microwave frequencies that is analogous to graphene and realize samples with ideal edges on a much more accessible millimeter length scale. The transmission at the Dirac point of this perfectly ordered structure enters a pseudodiffusive transport regime and becomes inversely proportional to the thickness of the sample, as predicted by theory [6]. We show that the termination of the surface has a profound effect on the coupling of microwaves to the structure. The measured transmission depends critically on the configuration of the edges. A distinct oscillation that modulates the transmission is observed for structures terminated with zigzag edges due to the excitation of different ''valleys'' in graphene. The amplitude of the oscillation is comparable to the transmission, and the oscillation is expected to persist for semi-infinite structures. The oscillation is completely absent for samples with a straight edge configuration. Our experiment establishes a direct link between the physics of electrons and photons in two-dimensional lattices with triangular symmetry. This provides a new and promising route to investigate other phenomena related to the conical singularities in the band structure of graphene that require samples with well-defined edges.

The feature that distinguishes graphene from other materials with a singularity in the band structure is that the singularities occur at the corners of the hexagonal Brillouin zone. There are two inequivalent corners or $\mathbf{K}$ points that are not connected by a reciprocal lattice vector, leading to two distinct $\mathbf{K}$ and $\mathbf{K}'$ valleys. Predictions for electrons in graphene that make use of these valleys, e.g., a valley-polarized beam splitter [12], are difficult to realize since the coupling of electron wave functions to different valleys depends critically on the edge termination and requires atomic scale engineering of individual carbon atoms. A simulation of an equivalent optical structure shows that an optical version of a valley-polarized beam splitter might be feasible experimentally [12].

The photonic crystal structure that we investigate is a triangular lattice of Al_2O_3 ceramic rods with a lattice constant $a = 8$ mm. The rods have a diameter of 5.1 mm and a dielectric constant $\epsilon = 9.8$ [13]. To ensure the two-dimensional nature of the material, the rods are 300 mm long, much longer than the lattice constant of the crystal

structure. The large dielectric constant of the rods and the judicious choice of other material parameters guarantee an isolated Dirac point in the band structure as shown in Fig. 1.

To experimentally probe the band structure we measured the transmitted amplitude, S_{21} of microwaves through a finite photonic crystal using a network analyzer (Agilent ENA E5071C) together with two identical horn antennas (Flann 18240-20). The horn antennas are equipped with 13.0 cm diameter Rexolite 1422 ($\epsilon = 2.53$) lens with a focal distance of 17.0 cm to create a parallel beam of microwaves. The measurements in Fig. 2 show the transmitted microwave amplitude S_{21}, through an 8-layer photonic crystal structure with straight edges (corresponding to armchair edges in the case of electronic graphene). For this configuration, normal incidence corresponds to the ΓM direction, and the ΓK direction is reached at an oblique angle of incidence. The black lines in the figure indicate the edges of the stop gaps and are derived from the band structure calculations of Fig. 1(b). At each frequency, the wave vector $\mathbf{k}$ is decomposed in a component parallel and perpendicular to the photonic crystal interface. Snell's law, which states that the wave-vector component parallel to the interface is conserved, can then be used to find a relation between external and internal angle. The crossing of the calculated bands, situated at a frequency of 17.2 GHz and an external angle of 45°, marks the conical singularity at the **K** point.

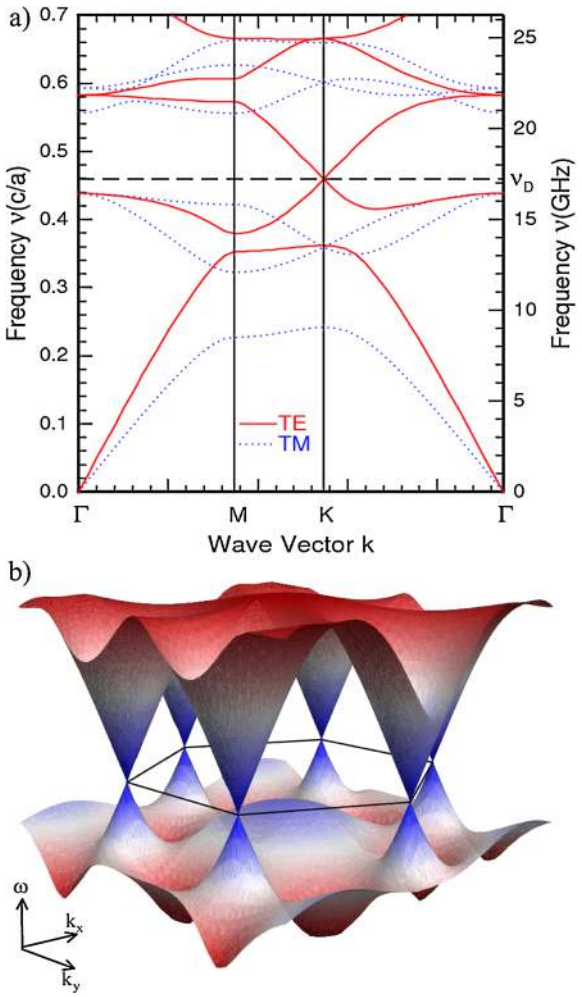

FIG. 1 (color online). Calculated photonic band structure of a triangular lattice of dielectric rods. The rods have a dielectric constant $\epsilon = 9.8$ and a radius-to-pitch ratio r/a of 0.32. (a) Conventional band structure $\nu(\mathbf{k})$ in dimensionless frequency units. An isolated conical singularity (Dirac point) can be identified between the second and third photonic band for TE-polarized waves. The singularity occurs at a dimensionless frequency $\nu = 0.458\ c/a$ at the **K** point on the corners of the hexagonal Brillouin zone. The right axis shows frequency units in GHz corresponding to the experimental structure with a lattice constant of 8 mm. (b) Three-dimensional surface plot of the second and third band of the band structure of photonic graphene as a function of two-dimensional wave vector. The figure shows the touching of the photonic bands at the six corners of the hexagonal Brillouin zone together with the conical dispersion for frequencies close to these Dirac points.

We first probe the consequence of a conical singularity in the band structure, by exciting a single **K** valley and varying the number of layers in the crystal. At the Dirac point, the transmission through the structure is predicted to scale diffusively as $1/L$, with L the crystal thickness. At this particular frequency, all modes responsible for the transmission through the structure are evanescent. The crucial difference between a structure with a singularity and a structure with a small band gap is that the decay length of the evanescent waves in the band gap is finite, while the wave that exactly excites the conical singularity

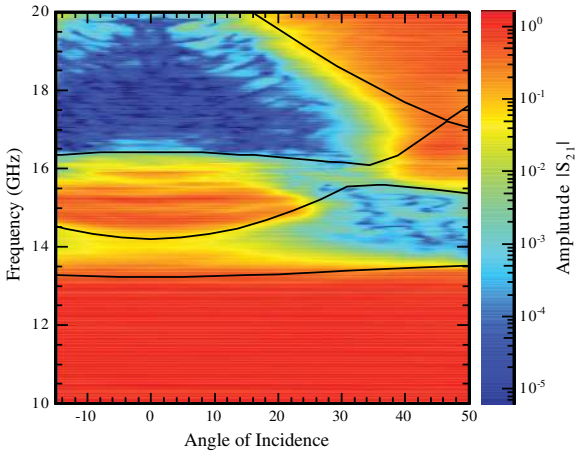

FIG. 2 (color). Measured transmission of TE-polarized microwaves through eight layers of photonic graphene as a function of angle of incidence. The color plot shows the transmitted amplitude $|S_{21}|$ as a function of external angle of incidence and frequency. Clearly visible are the blue regions with low transmission, corresponding to the stop gaps of the structure, and the red regions with high transmission, corresponding to propagating modes. The black lines show the edges of the stop gaps, derived from the calculated photonic band structure, and show that the Dirac point can be excited at an angle of incidence of 45° for a frequency close to 17.5 GHz.

has an infinite decay length. For monochromatic plane waves with a frequency corresponding to that of the Dirac point, the evanescent waves are given by $\exp(-\delta k_y x)$, where δk_y is the difference in transverse wave vector relative to the singular **K** point [6,7]. For an incident beam with a finite **k** spread or numerical aperture, the total transmission is obtained by integrating over a range of transverse wave vectors, that we denote as Δk:

$$T = \Gamma_0 \frac{W}{L}(1 - \exp[-\Delta k L]), \quad (1)$$

where L is the thickness of the crystal, W is the width of the crystal ($W \gg L$), and Γ_0 is a numerical prefactor [14], that reaches $1/\pi$ for ideal interfaces.

Figure 3 shows the measured transmission multiplied by the crystal thickness for an angle of incidence of 45° as a function of frequency. The stop gap between 13.5 and 15.5 GHz is easily identified. At a frequency of 17.6 GHz, indicated by the blue dashed arrows in the figure, the product of crystal thickness and transmission remains constant. At this frequency, the measured transmission in a perfectly ordered structure scales diffusively as $1/L$ as a direct consequence of the conical singularity in the band structure. In addition, at the Dirac frequency, the transmission as a function of angle should be a local maximum, since the states in the vicinity of the Dirac point are the only states contributing to the transmission. This is demonstrated by the inset of Fig. 3, which shows that the transmission at 17.6 GHz drops when tuning the angle of incidence away from 45°.

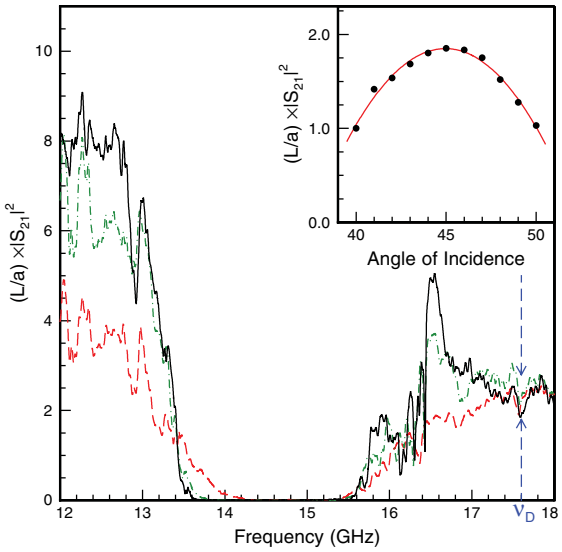

FIG. 3 (color). Transmission $|S_{21}|^2$ times the number of layers L/a as a function of frequency. The arrow close to 17.6 GHz indicates the position of the Dirac point. Measurements are shown for an angle of incidence of 45° for structures that are 20 rods wide, with straight edge termination and a thickness of 4 (red curve), 7 (green curve), and 9 layers of rods (black curve). The inset shows the measured value of $L|S_{21}|^2$ as a function of angle of incidence for a crystal with 9 layers and confirms that the Dirac point is excited at an angle of incidence of 45°.

For frequencies below the stop gap, the transmission is constant and close to 100%. The low reflectivity is consistent with the effective refractive index of the photonic crystal ($n_{\text{eff}} = 1.46$) and with the fact that the incoming TE-polarized wave is at an angle close to Brewster's angle ($\theta_B = 56°$). However, the measured transmission above the stop gap, away from the Dirac point, does not reach values close to 100% predicted by theory [14]. This is due to the finite size of the experimental detector, which does not collect the entire microwave beam exiting the crystal. This beam is enlarged by diffraction inside the photonic crystal.

The pseudodiffusive transport regime in photonic graphene is shown in Fig. 4 in more detail, by plotting the transmission at the Dirac frequency (17.6 GHz) versus the crystal thickness (L/a) on a log-log scale (open, red symbols). Figure 4 shows data for crystals with straight edges [Fig. 4(a)], and zigzag edges [Fig. 4(b)]. The solid red lines through the data are a fit to Eq. (1). The dashed lines represent the exact $1/L$ scaling behavior expected for large L. As can be seen, the experimental data approach $1/L$ scaling for the larger L/a values accessible in the experi-

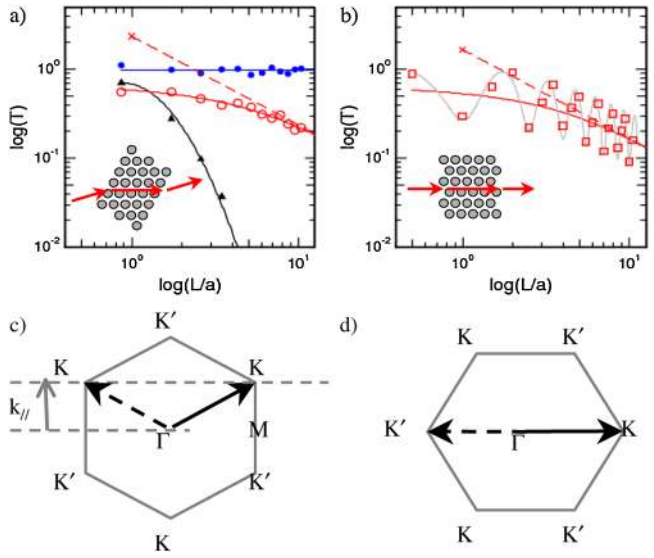

FIG. 4 (color online). Experimental observation of pseudodiffusive transport. The double logarithmic plots (a) and (b) show measured transmission as a function of crystal thickness for crystals terminated with straight and zigzag edges, respectively. The open symbols represent the measured transmission at the Dirac point. The solid, red lines through the data points are a fit to Eq. (1). The red dashed lines correspond to the asymptotic $1/L$ scaling behavior. For straight edges, the microwaves are incident at an angle of 45° [see inset of (a)] and excite only the singularities in one **K** valley (c). For zigzag edges, the microwaves at normal incidence [$\mathbf{k}_{\parallel} = \mathbf{0}$; see inset of (b)], excite both the **K** and the **K′** valley (d), leading to the characteristic oscillation where each additional layer adds a $2\pi/3$ phase shift. The gray line through the data is a fit of the data to Eq. (2). For comparison, (a) also shows the measured transmission below the first stop gap at 11 GHz (blue circles) and inside the stop gap at 14 GHz (black triangles), with lines to guide the eye.

ment ($L/a \gtrsim 5$). For comparison, Fig. 4(a) also shows the transmission at 11 GHz (blue circles), below the first stop gap, which is high and independent of the crystal thickness. The transmission inside the stop gap (black triangles in Fig. 4) decays exponentially with the number of layers and reaches a value below 1% for only 5 layers, due to the large contrast in dielectric constant which causes a strong interaction with light in our structures.

It is immediately apparent from the comparison of the data in Figs. 4(a) and 4(b) that the termination of the crystal edges, being either straight or zigzag, plays a crucial role. The nature of the interface determines the coupling of radiation to the photonic crystal structure. It is known that transport through graphene nanoribbons (a long narrow strip of graphene) is either insulating or metallic depending on the configuration of the edges [15,16]. Similar behavior has not yet been predicted or observed experimentally in electronic transport through graphene flakes because experimental structures do not have edges that are 100% zigzag or armchair terminated.

The essential difference between the zigzag and straight edge configuration is that the straight edge configuration leads to excitation of states in a single **K** valley, while the zigzag edges excite states belonging to both **K** valleys. This is illustrated in Figs. 4(c) and 4(d), which show the hexagonal Brillouin zone of the triangular lattice together with the wave vector of the light exciting one of the **K** points (solid arrow). For a crystal with straight edges, the parallel component of the wave vector $\mathbf{k}_{\parallel}$ of the incoming wave vector is nonzero, indicated by the horizontal dashed lines in Fig. 4(c). This wave is coupled, by reflection from each layer, to the wave indicated by the dashed arrow pointing to a **K** point belonging to the same **K** valley. This situation is fundamentally different from the zigzag terminated crystal. In this case, $\mathbf{k}_{\parallel} = \mathbf{0}$ and two **K** points on opposite sides of the hexagonal Brillouin are excited. These **K** points are not connected by a reciprocal lattice vector and both the **K** and **K**′ valleys are excited. This leads to an interference (gray line through the data), with a periodicity $2\pi/|\mathbf{K}|$, on top of the diffusive $1/L$ scaling. The transmission in this case can be expressed as

$$T = \Gamma_0 \frac{W}{L}(1 - \exp[-\Delta k L]) \cdot [(1 + g) + g\cos(|\mathbf{K}|L - \Delta\phi)]. \tag{2}$$

Here g is a parameter that controls the amplitude of the oscillating term, and $\Delta\phi$ is a phase difference to be determined. The gray line in Fig. 4(b) is a fit of the data to Eq. (2), yielding $g \approx 1.5$ and $\Delta\phi \approx \pi/3$. The profound oscillation is due to the excitation of the two different **K** valleys with comparable amplitude. We stress that this effect occurs due to the nature of the edges of the crystal and that the coupling between the valleys occurs via scattering at each layer of rods in the crystal. The amplitude of the oscillation is therefore always comparable to the transmission, independent of the crystal thickness.

The observation of a pseudodiffusive transport regime in a photonic analogue of graphene is one of the physical phenomena that can be observed in the photonic as well as in the electronic realization of graphene. By performing an experiment with samples with ideal edges of a well-defined configuration we were able to observe an oscillation with sample thickness related to the excitation of different **K** valleys; an effect that has not been observed for electrons in graphene. This holds promise for other experiments that probe the intriguing properties of these two-dimensional materials, such as the detection of the pseudospin $\frac{1}{2}$-Berry phase in a photonic crystal [17] or a valley-polarized beam splitter [12]. In the latter case, the photonic version of graphene holds promise to observe an effect which may not be possible in an electronic structure. Contrary to photons, there is little or no control over the wave vector of the incoming electrons. The availability of a photonic analogue enriches the field of graphene, making it possible to experimentally create and investigate *p-n* junctions with an arbitrarily sharp transition.

We thank Jos Disselhorst and Raymond Schouten for technical assistance, and Carlo Beenakker, Ruslan Sepkhanov, and Anton Akhmerov for scientific discussions. M. d. D. acknowledges financial support from the Dutch NWO and FOM organizations.

*Corresponding author.
mdedood@molphys.leidenuniv.nl

[1] A. K. Geim and K. S. Novoselov, Nature Mater. **6**, 183 (2007).
[2] P. R. Wallace, Phys. Rev. **71**, 622 (1947).
[3] K. S. Novoselov *et al.*, Nature (London) **438**, 197 (2005).
[4] Y. Zhang, Y.-W. Tan, H. L. Stormer, and P. Kim, Nature (London) **438**, 201 (2005).
[5] M. Plihal and A. A. Maradudin, Phys. Rev. B **44**, 8565 (1991).
[6] R. A. Sepkhanov, Ya. B. Bazaliy, and C. W. J. Beenakker, Phys. Rev. A **75**, 063813 (2007).
[7] S. Raghu and F. D. M. Haldane, Phys. Rev. A **78**, 033834 (2008).
[8] X. Zhang and Z. Liu, Phys. Rev. Lett. **101**, 264303 (2008).
[9] M. Gibertini *et al.*, Phys. Rev. B **79**, 241406(R) (2009).
[10] V. V. Cheianov, V. Fal'ko, and B. L. Altshuler, Science **315**, 1252 (2007).
[11] C. W. J. Beenakker, R. A. Sepkhanov, A. R. Akhmerov, and J. Tworzydło, Phys. Rev. Lett. **102**, 146804 (2009).
[12] J. L. Garcia-Pomar, A. Cortijo, and M. Nieto-Vesperinas, Phys. Rev. Lett. **100**, 236801 (2008).
[13] Anderman Ceramics, part No. ER 0197, http://www.earthwaterfire.com.
[14] R. A. Sepkhanov and C. W. J. Beenakker, Opt. Commun. **281**, 5267 (2008).
[15] K. Nakada, M. Fujita, G. Dresselhaus, and M. S. Dresselhaus, Phys. Rev. B **54**, 17954 (1996).
[16] L. Brey and H. A. Fertig, Phys. Rev. B **73**, 195408 (2006).
[17] R. A. Sepkhanov, J. Nilsson, and C. W. J. Beenakker, Phys. Rev. B **78**, 045122 (2008).